
AGC-DRIVE: A LARGE-SCALE DATASET FOR REAL-WORLD AERIAL-GROUND COLLABORATION IN DRIVING SCENARIOS

Yunhao Hou¹, Bochao Zou¹, Min Zhang², Ran Chen¹, Shangdong Yang², Yanmei Zhang²
Junbao Zhuo¹, Siheng Chen³, Jiansheng Chen¹, Huimin Ma^{1,*}

¹University of Science and Technology Beijing

²Xiamen NEVC Advanced Electric Powertrain Technology Innovation Center

³Shanghai Jiao Tong University

June 23, 2025

ABSTRACT

By sharing information across multiple agents, collaborative perception helps autonomous vehicles mitigate occlusions and improve overall perception accuracy. While most previous work focus on vehicle-to-vehicle and vehicle-to-infrastructure collaboration, with limited attention to aerial perspectives provided by UAVs, which uniquely offer dynamic, top-down views to alleviate occlusions and monitor large-scale interactive environments. A major reason for this is the lack of high-quality datasets for aerial-ground collaborative scenarios. To bridge this gap, we present AGC-Drive, the first large-scale real-world dataset for Aerial-Ground Cooperative 3D perception. The data collection platform consists of two vehicles, each equipped with five cameras and one LiDAR sensor, and one UAV carrying a forward-facing camera and a LiDAR sensor, enabling comprehensive multi-view and multi-agent perception. Consisting of approximately 120K LiDAR frames and 440K images, the dataset covers 14 diverse real-world driving scenarios, including urban roundabouts, highway tunnels, and on/off ramps. Notably, 19.5% of the data comprises dynamic interaction events, including vehicle cut-ins, cut-outs, and frequent lane changes. AGC-Drive contains 400 scenes, each with approximately 100 frames and fully annotated 3D bounding boxes covering 13 object categories. We provide benchmarks for two 3D perception tasks: vehicle-to-vehicle collaborative perception and vehicle-to-UAV collaborative perception. Additionally, we release an open-source toolkit, including spatiotemporal alignment verification tools, multi-agent visualization systems, and collaborative annotation utilities. The dataset and code are available at <https://github.com/PercepX/AGC-Drive>.

1 Introduction

Perception serves as a critical foundation for decision-making and safety in autonomous driving and multi-agent systems, especially in dynamic scenes with occlusions, long-range detection, and rapid response needs. To enhance perception completeness, existing cooperative perception systems mainly focus on Vehicle-to-Vehicle (V2V) [1, 2, 3][4, 5] and Vehicle-to-Infrastructure (V2I) [3, 4, 5][6, 7, 8][9, 10, 11] frameworks. V2V cooperative perception mitigates local occlusion issues by enabling information exchange among nearby vehicles. However, as all sensors remain at ground level, V2V systems struggle with dense traffic, occlusions, complex intersections, and limited perception range [6, 12]. Their performance is highly dependent on vehicle distribution and communication reliability. V2I cooperative perception utilizes roadside units (RSUs) to enhance sensing capabilities at critical points such as intersections and road segments [6, 8, 9]. Nevertheless, V2I systems face inherent limitations in deployment cost, fixed coverage, and adaptability to dynamic environments, making them unsuitable for large-scale open roads or rapidly evolving traffic scenarios.

Unlike V2V and V2I systems, Aerial-Ground Cooperative Perception (AGCP) introduces overhead Unmanned Aerial Vehicle (UAV)-based sensing, offering dynamic, adaptive, and high-altitude global perspectives to complement ground-based systems. UAVs can flexibly cover target areas, dynamically alleviate perception blind spots, enhance long-range target observation, and improve multi-object occlusion reasoning in complex traffic environments. This makes AGCP a

valuable complement to existing V2X systems, particularly in scenarios involving open roads, dynamic intersections, dense traffic, and emergency scenarios.

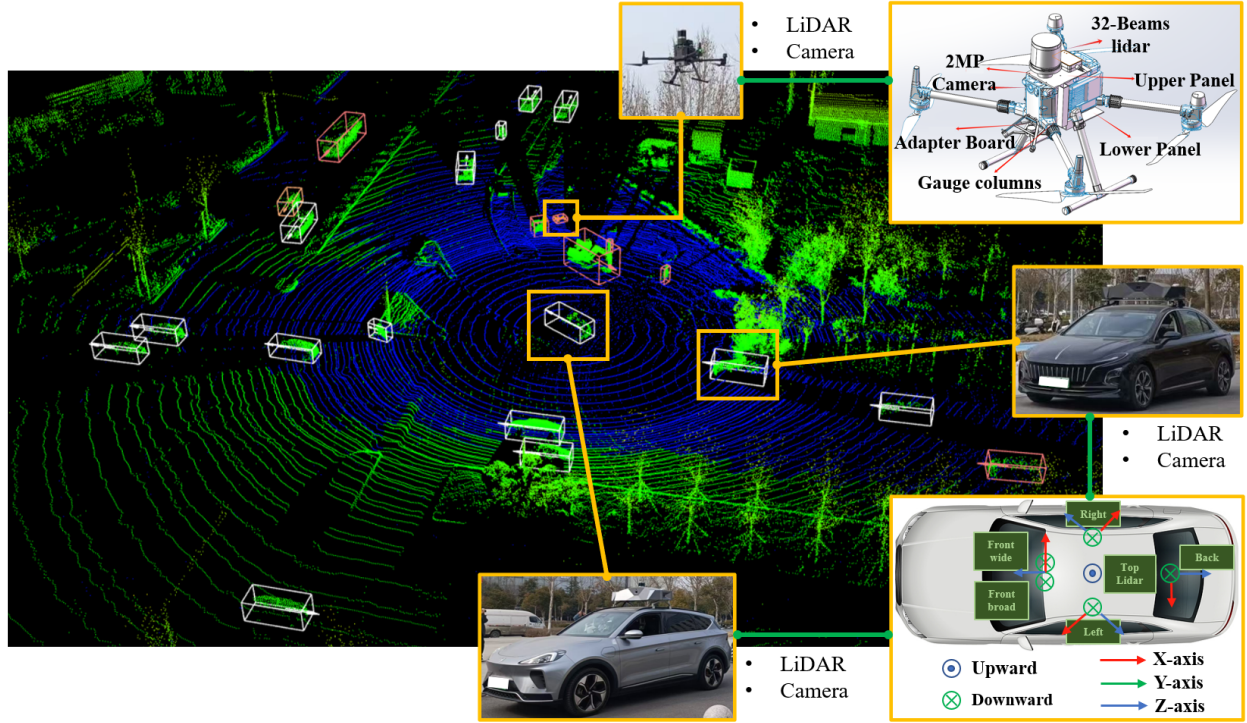


Figure 1: Collaborative data collection with two vehicles and a UAV. Each vehicle is equipped with one LiDAR and five cameras. The UAV carries a LiDAR and a camera system. The top-right inset shows the custom UAV sensor setup, and the bottom-right inset illustrates the vehicle’s sensor layout.

Although several datasets [13, 14, 15, 16, 12] have introduced UAVs into collaborative perception, they either focus on UAV-to-UAV cooperation [13, 14] or are collected in simulated environments [13, 14, 15, 12]. The only available real-world dataset [16] provides 2D annotations, but it is not collected in driving scenarios. Due to hardware limitations, none of these existing datasets include LiDAR-equipped UAVs. To bridge this gap, we introduce AGC-Drive, a dataset collected by a system consisting of two vehicles and one UAV (Figure 1) over approximately three months. From over 80 hours of collected data, we selected 400 sequences covering 14 scene categories. Each sequence contains 100 sets of data sampled at 10 Hz, with each set including 14 LiDAR frames and image frames, resulting in over 1.6M annotated 3D bounding boxes. Notably, we carefully designed the data collection routes to ensure a wide range of road conditions and vehicle interaction scenarios, covering high-risk environments such as urban roundabouts, highway tunnels, on/off ramps, and rural construction zones. Approximately 18.2% of the data involves dynamic events like vehicle cut-ins, cut-outs, and dense lane changes.

To support broad research in collaborative perception, we organized our dataset into two dedicated sub-collections: AGC-V2V for vehicle-to-vehicle collaboration, and AGC-VUC for vehicle-to-UAV collaboration. Additionally, to address the lack of UAV-based 3D object detection datasets using airborne LiDAR, we plan to introduce AGC-U3D, a carefully curated subset for UAV 3D object detection tasks.

Our main contributions are summarized as follows:

- We present AGC-Drive, the first real-world vehicle-vehicle-UAV collaborative perception dataset for driving scenarios, featuring time-synchronized multi-agent data collection and fused 360° ground and aerial views. It includes two sub-datasets: AGC-V2V and AGC-VUC.
- We provide over 1.6M annotated 3D bounding boxes for 13 categories, covering 120K LiDAR frames and 440K multi-view images, collected across 14 types of road environments and dynamic interaction scenarios such as lane changes and overtaking.
- We report benchmarks for two 3D perception tasks and release an open-source toolkit for spatiotemporal alignment, multi-agent visualization, and collaborative annotation.

2 Related work

With the rapid development of collaborative perception, an increasing number of high-quality datasets have been released. OPV2V [1] was the first collaborative perception dataset, featuring vehicle-to-vehicle (V2V) synthetic data. V2X-Sim [3] and V2XSet [4] extended this to vehicle-to-infrastructure (V2I) and V2V scenarios, but remained in simulated environments. DAIR-V2X [6] introduced the first large-scale, multi-modal, multi-view real-world V2I collaborative perception dataset. V2X-Seq [7] further contributed the first large-scale sequential collaborative dataset. Subsequently, five large-scale real-world datasets — V2V4Real [2], RCooper [8], TUMTraf-V2X [9], HoloVIC [10], and V2X-Real [5] have advanced research in vehicle-centric collaborative perception. Most recently, V2X-R [11] became the first dataset to incorporate 4D radar into collaborative perception.

Meanwhile, recent releases such as CoPerception-UAV [13] and UAV3D [14] reflect growing interest in incorporating UAVs into collaborative perception. However, both focus solely on UAV-to-UAV collaboration in simulated environments. More recently, V2U-COO [17] and Griffin [12] proposed aerial-ground collaborative datasets, but they are also synthetic and lack UAV LiDAR data due to hardware limitations. Although CoPeD [16] is a real-world aerial-ground collaborative dataset, it only provides monocular camera data with simple 2D annotations automatically generated by baseline models.

In contrast, AGC-Drive is a large-scale real-world dataset designed to support collaborative perception between aerial UAVs and ground vehicles. The UAV platforms are custom-designed and carefully equipped with LiDAR sensors. Table 1 summarizes the comparison with related datasets. It is worth noting that, similar to nuScenes [18], We annotate occlusion levels for each object, a detail often neglected in prior collaborative perception datasets. Moreover, our dataset covers 14 diverse scene categories under varying lighting conditions, with a day-to-night ratio of 8:2, significantly enhancing data diversity and robustness for perception tasks.

Table 1: A detailed comparison between representative single-UAV/cooperative perception datasets. Notes: V = Vehicle, I = Infrastructure, U = UAV. "V2V&I" indicates V2V and V2I, "V2V&U" indicates V2V and V2U. "MvCamera" denotes a Multi-view Camera System, "UAV-L" represents a UAV equipped with LiDAR, and "Driving" represents whether the dataset is collected in autonomous driving scenarios.

Mode	Dataset	Year	Source	Agent	Sensor	scenario types	3D boxes	Classes	MvCams	Driving	UAV-L
V2V	OPV2V [1]	2022	Sim	Veh	C & L	6	230K	1	✓	✓	×
	V2V4Real [2]	2023	Real	Veh	C & L	-	240K	5	✓	✓	×
V2I	DAIR-V2X [6]	2022	Real	Veh & Inf	C & L	-	464K	10	×	✓	×
	V2X-Seq [7]	2023	Real	Veh & Inf	C & L	-	-	9	×	✓	×
	Rcooper [8]	2024	Real	Veh & Inf	C & L	-	-	10	×	✓	×
	TUMTraf-V2X [9]	2024	Real	Veh & Inf	C & L	-	29.3K	8	×	✓	×
	HoloVIC [10]	2024	Real	Veh & Inf	C & L	-	11.4M	3	×	✓	×
	V2X-R [11]	2025	Real	Veh & Inf	C & L & R	-	-	5	×	✓	×
V2V&I	V2X-Sim [3]	2022	Sim	Veh & Inf	C & L	-	26.6K	1	✓	✓	×
	V2XSet [4]	2022	Sim	Veh & Inf	C & L	5	230K	1	✓	✓	×
	V2X-Real [5]	2024	Real	Veh & Inf	C & L	-	1.2M	10	✓	✓	×
UAV	VisDrone [19]	2018	Real	UAV	C	-	10.2K	10	×	×	×
	UAVDT [20]	2018	Real	UAV	C	-	841.5K	3	✓	✓	×
U2U	CoPerception-UAV [13]	2023	Sim	UAV	C	-	1.6M	21	✓	✓	×
	UAV3D [14]	2023	Sim	UAV	C	-	3.3M	17	✓	✓	×
V2U	V2U-COO [17]	2024	Sim	Veh & UAV	C	-	-	4	×	✓	×
	CoPeD [16]	2024	Real	Veh & UAV	C & L	2	×	1	×	×	×
	Griffin [12]	2025	Sim	Veh & UAV	C & L	4	-	3	✓	✓	×
V2V&U	AGC-Drive(Ours)	2025	Real	Veh & UAV	C & L & R	14	1.6M	13	✓	✓	✓

3 The AGC-Drive Dataset

To bridge collaborative vehicle-to-vehicle and aerial-ground perception research and to establish a comprehensive 3D traffic perception framework, we present AGC-Drive — a large-scale, multimodal, multi-view, and multi-scenario dataset featuring well-annotated 3D bounding boxes for innovative research on UAV-vehicle collaboration. In this section, we describe the data acquisition devices, coordinate system design, multi-sensor calibration, scene selection strategies, detailed data collection, annotation processes and pose refinement, as well as privacy protection considerations.

3.1 Setup

Sensors. The data acquisition system consists of two instrumented vehicles and one UAV: a) Vehicle-mounted sensors. Each vehicle is equipped with a 128-beam LiDAR and five high-resolution cameras. Notably, the front-facing cameras are configured with two different focal lengths to capture both detailed road surface information and broader traffic scene context; b) UAV-mounted sensors. The UAV platform is based on a modified DJI M350 RTK, equipped with a 32-beam LiDAR and a high-resolution downward-facing camera. The sensor configuration is illustrated in Fig.1, with detailed specifications summarized in Table 2.

Table 2: Key Sensor Specifications in AGC-Drive.

Agent	Sensor	Sensor Model	Detail
2*Vehicle	LiDAR	RoboSense Ruby Plus(*1)	128 beams, 10Hz capture frequency, 360°horizontal FOV, -25°to +15°vertical FOV, < 200m range
	Camera	Sensing Cmaera(*5)	front-wide: SG8S-AR0820C-5300-G2A-Hxxx, 8MP, HFOV30°, front-broad: SG8S-AR0820C-5300-G2A-Hxxx, 8MP, HFOV120°, left&right: SG2-AR0231C-0202-GMSL-Hxxx, 2MP, HFOV100°, back: SG2-AR0233C-5200-G2A-Hxxx, 2mp, HFOV121°
	GPS&IMU	Intelligent Car Built-in GPS System(*1)	100HZ
UAV	LiDAR	RoboSense Helios32(*1)	32 beams, 10Hz capture frequency, 360°horizontal FOV, -55°to +15°vertical FOV,< 150m range
	Camera	USB Camera(*1)	front: RER-USBGS1200P02, 2MP, HFOV120°
	GPS&IMU	DJI M350 RTK Built-in GPS System(*1)	GPS + GLONASS + BeiDou + Galileo, 100HZ

Coordinate System. The AGC-Drive dataset defines four types of coordinate systems: LiDAR coordinate system, camera coordinate system, image coordinate system, and world coordinate system. Each agent is equipped with its own LiDAR and camera coordinate systems. The camera coordinate system is aligned to the corresponding LiDAR frame via a camera-to-LiDAR calibration process. Then, the pose information from each agent’s GPS/IMU is used as an initial transformation, and all LiDAR coordinate systems are registered to a unified world coordinate system through point cloud registration. The calibration results are illustrated in Fig. 1.

Calibration. To ensure accurate spatial alignment between the LiDAR point cloud and multiple cameras, we perform extrinsic calibration for each camera with respect to the LiDAR sensor. First, the intrinsic parameters of each camera are obtained using a standard checkerboard calibration. Then, we collect synchronized images and LiDAR data of a calibration target visible in both modalities. 3D-2D correspondences are established by detecting feature points in the images and extracting the corresponding points from the LiDAR point cloud. Finally, the extrinsic transformation matrices are estimated using a Perspective-n-Point (PnP) algorithm [21], followed by visual verification through point cloud projection onto the image plane.

Scenario Planning. To ensure the representativeness and utility of our dataset, we follow the Task-driven Scenario Taxonomy [22] and Operational Design Domain (ODD) definitions [23]. We also reference popular autonomous driving datasets such as Waymo Open Dataset [24] and nuScenes [18]. Scenarios are designed based on common driving tasks including lane keeping, lane changing, car-following, intersection crossing, roundabout navigation, construction detours, and ramp merging. Combined with ODD, they are categorized into urban, highway, and rural environments, further covering typical cases like straight roads, curves, intersections, construction zones, tunnels, and frequent lane changes. In total, 14 representative driving scenarios are constructed (Fig. 2), providing comprehensive coverage for both routine and high-risk conditions.

3.2 Data Acquisition

Collection. We deployed two equipped vehicles and a UAV operated by professional pilots to collect synchronized data. Each agent locally records data frames, with timestamps aligned to its GPS time, achieving unified time sources across all agents. Data were collected along predefined routes over 2 months under varying day and night conditions, accumulating over 80 hours of driving logs. From the raw data, we curated 400 representative segments (10s each) across 14 scenarios, resulting in 120K LiDAR frames and 440K camera images with annotations. Keyframes were extracted at 10 Hz to construct AGC-V2V, while segments involving UAV participation were used to create AGC-VUC for vehicle-UAV collaborative perception tasks. Additionally, we plan to extract UAV LiDAR data to support UAV-based 3D perception research.

Annotation. We customized an annotation platform based on the open-source tool Xtreme1 [25] to meet the specific needs of our dataset. A team of 100 annotators was recruited, with multiple rounds of expert review to ensure annotation quality. On average, each frame underwent two rounds of review and revision. Our dataset provides 3D annotations

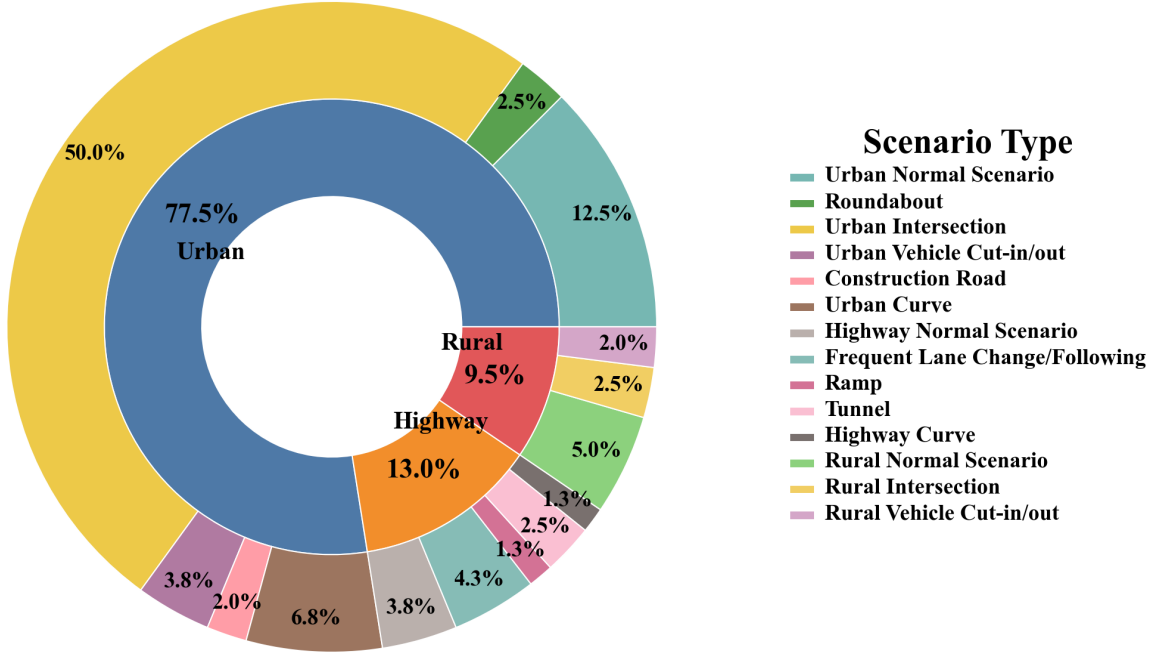


Figure 2: Distribution of Driving Environment and Scenario Types. The inner ring categorizes the data into three primary driving environments: Urban (77.5%), Highway (13.0%), and Rural (9.5%). The outer ring further subdivides these environments into specific scenario types.

for 13 object categories, including pedestrian, rider, motorcycle, bicycle, tricycle, car, truck, van, bus, road obstacles, traffic cones, and traffic signs. Each object is labeled with a 9-DoF 3D bounding box, consisting of (x, y, z) for the box center, (l, w, h) for size, and roll, pitch, yaw for orientation. Furthermore, each 3D bounding box is projected onto the corresponding camera images to generate two types of 2D annotations: an 8-vertex 2D polygon representing the projected 3D box corners, and a 4-vertex 2D rectangle corresponding to the minimum enclosing rectangle of the projected box. Additionally, each object is assigned one of three occlusion levels: visible (0–20%), partially occluded (20–50%), or heavily occluded (over 50%).

Relative Pose. In this work, we estimate the relative poses between three agents: two vehicles and a UAV, using their respective GPS, IMU, and LiDAR data. Initially, GPS and IMU data provide the initial pose estimates for each agent. These initial poses serve as the starting input for the Iterative Closest Point (ICP) algorithm [26]. The ICP algorithm is then used to perform pairwise point cloud registration, aligning the LiDAR point clouds of the vehicles and UAV. This process calculates the relative poses between each pair of agents based on the aligned point clouds. After ICP registration, the relative poses are refined and corrected to improve accuracy. Finally, the corrected poses are transformed into the ego vehicle’s coordinate frame, ensuring consistent spatial alignment across all agents. This method enables robust and accurate relative pose estimation, which is crucial for multi-agent cooperative perception tasks.

Privacy Protection. Prior to public release, all sensitive information in the dataset was anonymized. We removed all location metadata, including road names, map data, and GPS information, to comply with legal and ethical regulations. In addition, a professional annotation tool was used to blur potential privacy-related content, such as traffic signs, license plates, and human faces, to ensure protection of personal privacy.

4 Task And Benchmark

We benchmark AGC-Drive on collaborative 3D object detection tasks, including vehicle-to-vehicle cooperation, vehicle-UAV cooperative(VUC) 3D object detection.

Dataset Format and Split. Our AGC-Drive dataset follows the OPV2V [1] format, containing 14 road types with multiple scenes per type (distribution shown in Fig. 2). Each scene consists of 100 groups of synchronized multi-agent

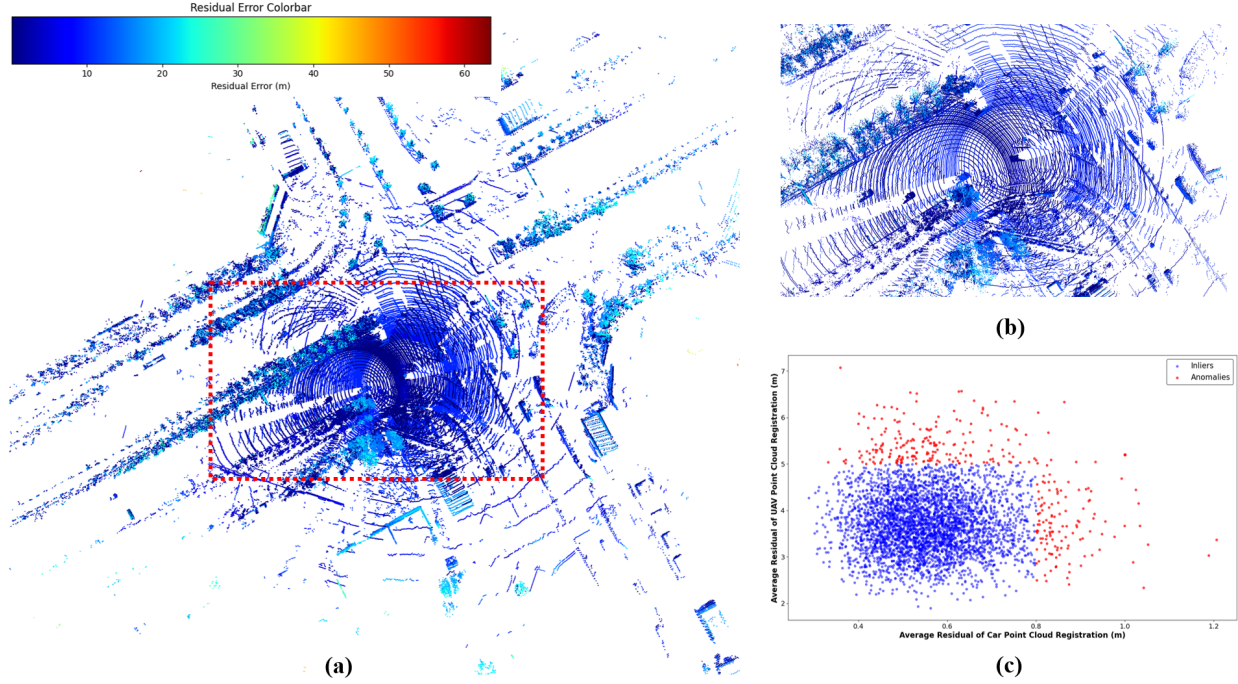


Figure 3: (a) Point-to-point residual heatmap of the registration results. As indicated by the color bar, colors transition from blue to red, representing registration accuracy from high to low. (b) A zoomed-in view of the dense object region highlighted by the dashed box in (a). (c) Scatter plot of the average residuals for 4000 randomly sampled points, where both the drone and vehicle point clouds are registered to the ego vehicle’s point cloud.

data, collected by 1 drone and 2 vehicles equipped with a total of 14 sensors. In total, we collect 400 scenes, with 320 for training, 90 for validation, and 90 for testing.

Input and Ground Truth. For each agent, the input includes synchronized LiDAR point clouds captured at 10 Hz. The shared data from neighboring vehicles are fused in the bird’s eye view (BEV) space for cooperative perception. The ground truth consists of 9-DoF 3D bounding boxes annotated for 13 categories (car, truck, pedestrian, cyclist, etc.) with additional occlusion status labels (visible, partially occluded, heavily occluded) following the nuScenes convention [18].

Benchmark Frameworks. We benchmark six representative cooperative perception frameworks, all of which adopt PointPillars [27] as the detection backbone for a fair comparison:

- **Upper-bound:** Directly shares raw point cloud data among agents before feature extraction.
- **Lower-bound:** Independently detects objects and shares detection results among agents.
- **V2VNet** [1]: A multi-agent cooperative detection framework using intermediate feature fusion.
- **Cobevt** [28]: A cooperative BEV semantic segmentation framework based on sparse transformers, employing a feature aggregation module (FAX) to effectively fuse multi-view and multi-agent features.
- **Where2comm** [13]: A communication-efficient cooperative perception framework that guides agents to share only spatially sparse yet perception-critical information using a spatial confidence map, achieving a balance between perception performance and communication bandwidth.
- **V2X-ViT** [4]: A recent transformer-based cooperative perception framework leveraging BEV feature fusion with attention mechanisms.

Experiments Details. For all tasks, the models are adapted to support the AGC-V2V and AGC-VUC data format and sensor configurations. We adopt a unified BEV (Bird’s Eye View) representation. The perception range is set to $[-150\text{ m}, 150\text{ m}]$ along both the X and Y axes. All baseline models were trained with a batch size of 4 for 40 epochs, with a per-GPU batch size of 1 on a computing server equipped with 8 Nvidia L40 GPUs. We use the Adam optimizer with an initial learning rate of 0.001 and apply a cosine learning rate schedule. Each training run takes approximately 6 hours.

Finally, we report standard evaluation metrics following the protocols of nuScenes [18] and OPV2V [1], including mAP@0.5 and mAP@0.7 for 3D object detection, along with Δ_{UAV} , to quantify the impact of the UAV’s participation on the perception performance of the cooperative system.

4.1 Benchmark for V2V 3D object detection

Problem Definition and AGC-V2V. The goal of this task is to perform cooperative 3D object detection by leveraging information from multiple connected vehicles to enhance perception performance, especially in challenging scenarios such as long-range detection and occlusions. We construct the AGC-V2V benchmark by selecting collaborative scenes from the AGC-Drive dataset where two vehicles participate without UAV involvement. Each vehicle is equipped with a LiDAR sensor and five cameras. A total of 400 scenes, comprising 80K frames, are included for this benchmark.

Quantitative Results. Table 3 reports the results of V2V 3D object detection on AGC-V2V. It is unsurprising that the Upper-bound early fusion achieves superior results across all metrics, given its access to fully aggregated information. The overall performance of all frameworks remains relatively low, especially for feature-sensitive intermediate fusion methods, primarily due to the lack of handling for time delays and pose estimation errors. The Lower-bound late fusion performs the worst, due to the accumulation of multiple errors introduced during the collaborative fusion process.

Table 3: 3D Detection Performance (%) on AGC-V2V.

Co-Mode	Model	mAP@0.5	mAP@0.7
Late	Lower-bound	26.6	12.2
Intermediate	V2VNet [1]	27.2	14.1
	Cobevt [28]	28.6	14.9
	Where2comm [13]	34.8	22.5
	V2X-ViT [4]	32.7	18.7
Early	Upper-bound	58.2	43.1

Qualitative results. Figure 4 presents qualitative 3D object detection results of four intermediate collaborative baselines under several challenging scenarios, including highway tunnel occlusions, intersection occlusions with long-range targets, and complex road occlusions. We see that V2V cooperative perception effectively alleviates the challenges posed by long-range perception and occlusions. However, due to unaddressed pose errors and time delays, the localization accuracy of the predicted results is lower than that of single-vehicle detection, leading to a decline in overall performance metrics.

4.2 Benchmark for VUC3D object cooperation

Problem Definition and AGC-VUC. This task aims to improve 3D object detection by leveraging the complementary perception capabilities of ground vehicles and UAVs. Unlike traditional V2V cooperation, the UAV provides a global top-down view that enhances occlusion handling and long-range detection. To support this, we construct the AGC-VUC benchmark by selecting cooperative scenarios in AGC-Drive that involve two vehicles and one UAV. Each scenario lasts approximately 10 seconds, sampled at 10Hz, resulting in 200 cooperative sequences.

Quantitative Results. Table 4 presents the benchmark results after incorporating the UAV into the cooperative system. Here, we add a new column, denoted as Δ_{UAV} , to quantify the impact of the UAV’s participation on the perception performance of the cooperative system. It can be observed that the introduction of the UAV improves the performance of all cooperative frameworks across all metrics, except for the Lower-bound. Among them, the Upper-bound achieves the largest improvement, with a Δ_{UAV} value of +3.3.

Qualitative results. Figure 5 presents qualitative 3D object detection results of four intermediate collaborative baselines under several challenging scenarios. By comparing the visualization results with V2V baselines, we observe that integrating UAV perspective data effectively improves the ego vehicle’s perception performance, particularly for distant and occluded objects in a larger area of the same scene.

5 Limitations

Since this is the first attempt to mount a vehicle-mounted LiDAR sensor on a UAV for real-time object detection data collection, we carefully considered factors such as the UAV’s flight altitude, the LiDAR’s weight, and the blind zone

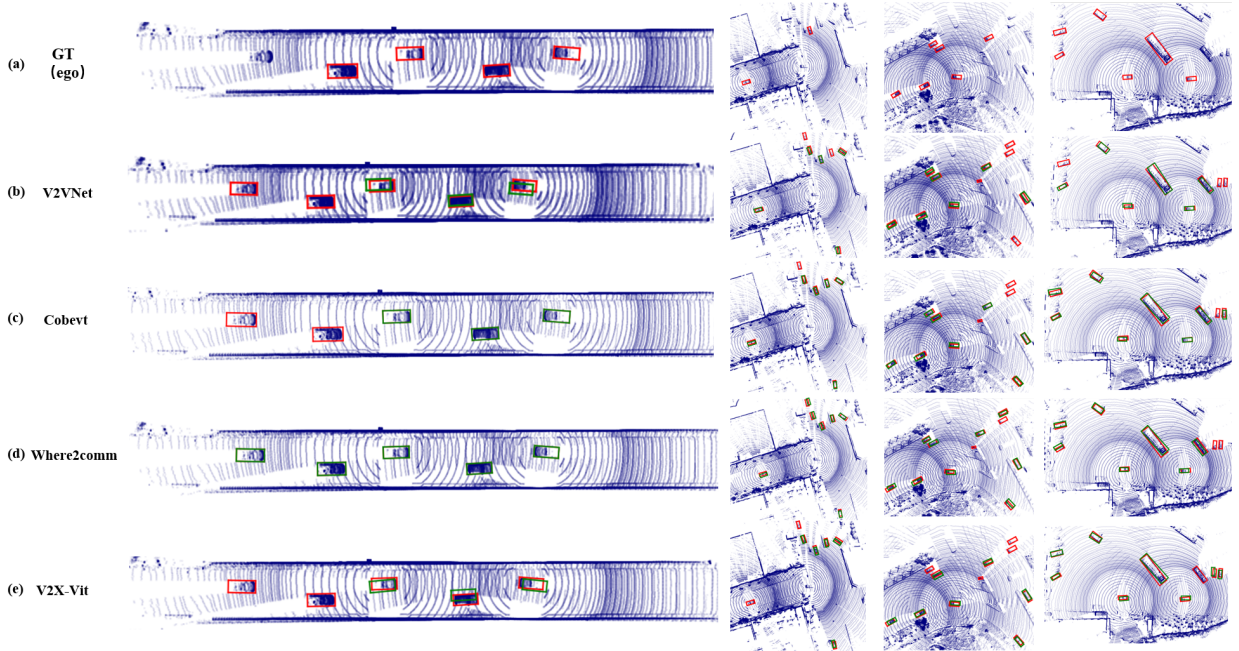


Figure 4: Point cloud visualization of V2V cooperative object detection results on the AGC-V2V dataset. Green bounding boxes denote predicted objects, and red bounding boxes indicate ground truth annotations.

Table 4: 3D Detection Performance (%) on AGC-VUC.

Co-Mode	Model	mAP@0.5	mAP@0.7	Δ_{UAV}
Late	Lower-bound	24.9	11.6	-1.0
Intermediate	V2VNet [1]	28.5	14.9	+1.0
	Cobevt [28]	30.7	16.1	+1.6
	Where2comm [13]	36.4	23.1	+1.1
	V2X-ViT [4]	33.9	18.4	+0.4
Early	Upper-bound	61.3	46.5	+3.3

beneath the UAV caused by the LiDAR’s vertical field of view during the system design. However, there were still some aspects that were insufficiently addressed. In our experimental validation, although the point cloud data collected from the UAV perspective contributed to a more comprehensive perception of large-scale scenes, its relatively sparse nature limited its ability to provide fine-grained perception assistance for collaborative tasks. We have recognized this issue and plan to explore potential upgrades or replacements for the UAV-mounted LiDAR before conducting large-scale dataset collection in the future. Our goal is for the UAV’s point clouds not only to enhance large-scale scene awareness but also to offer more detailed, object-level perception information to support ground vehicles.

6 Discussion And Conclusion

We present AGC-Drive, a large-scale, multimodal dataset for collaborative perception between aerial UAVs and ground vehicles, collected in real-world environments. Compared to existing aerial-ground collaborative perception datasets, AGC-Drive is built upon real-world data with annotated 3D bounding boxes. Notably, it includes point cloud data collected from the UAV perspective, enabling collaborative perception at scene level. We further adapt several representative collaborative perception frameworks to our dataset and provide comprehensive benchmark results. It is worth noting that we retain data containing time delays and pose errors caused by point cloud registration, in order to better reflect the challenges encountered in real-world scenarios. All associated resources, including benchmark code, annotation tools, pose correction toolkits, and the complete AGC-Drive dataset, are publicly released. In addition, our raw data includes synchronized multi-modal signals such as 4D radar, in-cabin steering wheel status, brake signals, and driver-facing cameras. We hope this work will benefit the broader community working on aerial-ground collaborative

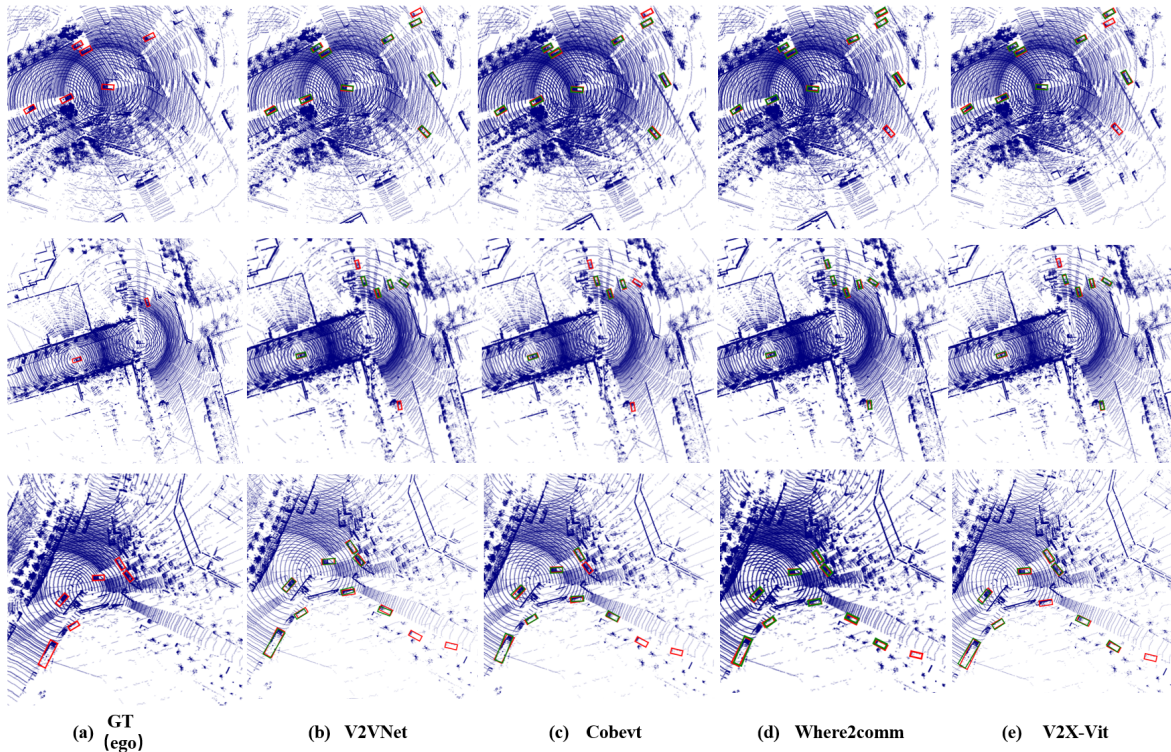


Figure 5: Point cloud visualization of VUC object detection results on the AGC-VUC dataset. Green bounding boxes denote predicted objects, and red bounding boxes indicate ground truth annotations.

perception. Future work includes refining the UAV LiDAR dataset, collecting larger-scale datasets with dense multi-UAV point cloud collaboration scenarios, expanding data collection under various weather conditions, and annotating for additional vision-action tasks. However, misuse of the dataset or models trained on it could lead to overreliance on imperfect perception systems in safety-critical applications, especially given the inclusion of time delays and pose errors that reflect real-world challenges. This could potentially result in incorrect decisions in autonomous driving scenarios. We emphasize the importance of responsible use, adherence to ethical guidelines, and the implementation of safeguards to mitigate such risks.

References

- [1] Runsheng Xu, Hao Xiang, Xin Xia, Xu Han, Jinlong Li, and Jiaqi Ma. Opv2v: An open benchmark dataset and fusion pipeline for perception with vehicle-to-vehicle communication. In *2022 International Conference on Robotics and Automation (ICRA)*, page 2583–2589. IEEE Press, 2022.
- [2] Runsheng Xu, Xin Xia, Jinlong Li, Hanzhao Li, Shuo Zhang, Zhengzhong Tu, Zonglin Meng, Hao Xiang, Xiaoyu Dong, Rui Song, et al. V2v4real: A real-world large-scale dataset for vehicle-to-vehicle cooperative perception. In *Proceedings of the IEEE/CVF Conference on Computer Vision and Pattern Recognition*, pages 13712–13722, 2023.
- [3] Yiming Li, Dekun Ma, Ziyang An, Zixun Wang, Yiqi Zhong, Siheng Chen, and Chen Feng. V2x-sim: Multi-agent collaborative perception dataset and benchmark for autonomous driving. *IEEE Robotics and Automation Letters*, 7(4):10914–10921, 2022.
- [4] Runsheng Xu et al. V2x-vit: Vehicle-to-everything cooperative perception with vision transformer. In *ECCV Proceedings*, 2022.
- [5] Hao Xiang, Zhaoliang Zheng, Xin Xia, Runsheng Xu, Letian Gao, Zewei Zhou, Xu Han, Xinkai Ji, Mingxi Li, Zonglin Meng, et al. V2x-real: a large-scale dataset for vehicle-to-everything cooperative perception. In *European Conference on Computer Vision*, pages 455–470. Springer, 2024.
- [6] Haibao Yu, Yizhen Luo, Mao Shu, Yiyi Huo, Zebang Yang, Yifeng Shi, Zhenglong Guo, Hanyu Li, Xing Hu, Jirui Yuan, et al. Dair-v2x: A large-scale dataset for vehicle-infrastructure cooperative 3d object detection. In *Proceedings of the IEEE/CVF Conference on Computer Vision and Pattern Recognition*, pages 21361–21370, 2022.
- [7] Haibao Yu, Wenxian Yang, Hongzhi Ruan, Zhenwei Yang, Yingjuan Tang, Xu Gao, Xin Hao, Yifeng Shi, Yifeng Pan, Ning Sun, et al. V2x-seq: A large-scale sequential dataset for vehicle-infrastructure cooperative perception and forecasting. In *Proceedings of the IEEE/CVF Conference on Computer Vision and Pattern Recognition*, pages 5486–5495, 2023.
- [8] Ruiyang Hao, Siqi Fan, Yingru Dai, Zhenlin Zhang, Chenxi Li, Yuntian Wang, Haibao Yu, Wenxian Yang, Yuan Jirui, and Zaiqing Nie. Rcooper: A real-world large-scale dataset for roadside cooperative perception. In *Proceedings of the IEEE/CVF Conference on Computer Vision and Pattern Recognition (CVPR)*, pages 22347–22357, 2024.
- [9] Walter Zimmer, Gerhard Arya Wardana, Suren Sritharan, Xingcheng Zhou, Rui Song, and Alois C Knoll. Tumtraf v2x cooperative perception dataset. In *Proceedings of the IEEE/CVF conference on computer vision and pattern recognition*, pages 22668–22677, 2024.
- [10] Cong Ma, Lei Qiao, Chengkai Zhu, Kai Liu, Zelong Kong, Qing Li, Xueqi Zhou, Yuheng Kan, and Wei Wu. Holovic: Large-scale dataset and benchmark for multi-sensor holographic intersection and vehicle-infrastructure cooperative. In *Proceedings of the IEEE/CVF Conference on Computer Vision and Pattern Recognition*, pages 22129–22138, 2024.
- [11] Xun Huang, Jinlong Wang, Qiming Xia, Siheng Chen, Bisheng Yang, Cheng Wang, and Chenglu Wen. V2x-r: Cooperative lidar-4d radar fusion for 3d object detection with denoising diffusion. *arXiv preprint arXiv:2411.08402*, 2024.
- [12] Jiahao Wang, Xiangyu Cao, Jiaru Zhong, Yuner Zhang, Haibao Yu, Lei He, and Shaobing Xu. Griffin: Aerial-ground cooperative detection and tracking dataset and benchmark. *arXiv preprint arXiv:2503.06983*, 2025.
- [13] Yue Hu, Shaoheng Fang, Zixing Lei, Yiqi Zhong, and Siheng Chen. Where2comm: Communication-efficient collaborative perception via spatial confidence maps. *Advances in neural information processing systems*, 35:4874–4886, 2022.
- [14] Rajshekhar Sunderraman, Jonathan Shihao Ji, et al. Uav3d: A large-scale 3d perception benchmark for unmanned aerial vehicles. *Advances in Neural Information Processing Systems*, 37:55425–55442, 2024.
- [15] Zhechao Wang, Peirui Cheng, Minxing Chen, Pengju Tian, Zhirui Wang, Xinming Li, Xue Yang, and Xian Sun. Drones help drones: A collaborative framework for multi-drone object trajectory prediction and beyond. *Advances in Neural Information Processing Systems*, 37:64604–64628, 2024.
- [16] Yang Zhou, Long Quang, Carlos Nieto-Granda, and Giuseppe Loianno. Coped-advancing multi-robot collaborative perception: A comprehensive dataset in real-world environments. *IEEE Robotics and Automation Letters*, 9(7):6416–6423, 2024.
- [17] Yuchao Wang, Zhirui Wang, Peirui Cheng, Pengju Tian, Ziyang Yuan, Jing Tian, Wensheng Wang, and Liangjin Zhao. Uvcnpnet: A uav-vehicle collaborative perception network for 3d object detection. *IEEE Transactions on Geoscience and Remote Sensing*, 2025.
- [18] Holger Caesar, Varun Bankiti, Alex H Lang, Sourabh Vora, Venice Erin Liong, Qiang Xu, Anush Krishnan, Yu Pan, Giancarlo Baldan, and Oscar Beijbom. nuscenes: A multimodal dataset for autonomous driving. In *Proceedings of the IEEE/CVF conference on computer vision and pattern recognition*, pages 11621–11631, 2020.
- [19] Pengfei Zhu, Longyin Wen, Dawei Du, Xiao Bian, Heng Fan, Qinghua Hu, and Haibin Ling. Detection and tracking meet drones challenge. *IEEE Transactions on Pattern Analysis and Machine Intelligence*, 44(11):7380–7399, 2021.
- [20] Dawei Du, Yuankai Qi, Hongyang Yu, Yifan Yang, Kaiwen Duan, Guorong Li, Weigang Zhang, Qingming Huang, and Qi Tian. The unmanned aerial vehicle benchmark: Object detection and tracking. In *Proceedings of the European conference on computer vision (ECCV)*, pages 370–386, 2018.
- [21] Martin A Fischler and Robert C Bolles. Random sample consensus: a paradigm for model fitting with applications to image analysis and automated cartography. *Communications of the ACM*, 24(6):381–395, 1981.

- [22] International Organization for Standardization. ISO 34502:2022 Road vehicles — Test scenarios for automated driving systems, 2022. Available: <https://www.iso.org/standard/77109.html>.
- [23] Robert Trypuz, Piotr Kulicki, and Mirek Sopek. Ontology of autonomous driving based on the sae j3016 standard. *Semantic Web*, 15(5):1837–1862, 2024.
- [24] Pei Sun, Henrik Kretzschmar, Xerxes Dotiwalla, Aurelien Chouard, Vijaysai Patnaik, Paul Tsui, James Guo, Yin Zhou, Yuning Chai, Benjamin Caine, et al. Scalability in perception for autonomous driving: Waymo open dataset. In *Proceedings of the IEEE/CVF conference on computer vision and pattern recognition*, pages 2446–2454, 2020.
- [25] LF AI & Data Foundation. Xtreme1 - the next gen platform for multisensory training data, 2023. Software available from <https://github.com/xtreme1-io/xtreme1/>.
- [26] Paul J Besl and Neil D McKay. Method for registration of 3-d shapes. In *Sensor fusion IV: control paradigms and data structures*, volume 1611, pages 586–606. Spie, 1992.
- [27] Alex H Lang, Sourabh Vora, Holger Caesar, Lubing Zhou, Jiong Yang, and Oscar Beijbom. Pointpillars: Fast encoders for object detection from point clouds. In *Proceedings of the IEEE/CVF conference on computer vision and pattern recognition*, pages 12697–12705, 2019.
- [28] Hao Xiang Wei Shao Bolei Zhou Jiaqi Ma Runsheng Xu, Zhengzhong Tu. Cobevt: Cooperative bird’s eye view semantic segmentation with sparse transformers. In *Conference on Robot Learning (CoRL)*, 2022.